JGR Oceans

RESEARCH ARTICLE
10.1029/2019JC015862

A Lagrangian View of Trace Elements and Isotopes in the North Pacific

Christopher T. Hayes[1], Jessica N. Fitzsimmons[2], Laramie T. Jensen[2], Nathan T. Lanning[2], Mariko Hatta[3], David McGee[4], and Edward A. Boyle[4]

[1]School of Ocean Science and Engineering, University of Southern Mississippi, Stennis Space Center, MS, USA, [2]Department of Oceanography, Texas A&M University, College Station, TX, USA, [3]Department of Oceanography, University of Hawaii, Honolulu, HI, USA, [4]Department of Earth, Atmospheric and Planetary Sciences, Massachusetts Institute of Technology, Cambridge, MA, USA

Key Points:
- A suite of 11 trace elements was analyzed in one patch of surface water at twice-daily resolution for 12 days near Station ALOHA
- No diel patterns could be resolved; daily variations are suggestive of active biogeochemical cycling in this oligotrophic region
- Interannual variations, in particular for Pb, and nutrient-trace element stoichiometry with respect to prior observations was assessed

Correspondence to:
C. T. Hayes,
christopher.t.hayes@usm.edu

Citation:
Hayes, C. T., Fitzsimmons, J. N., Jensen, L. T., Lanning, N. T., Hatta, M., McGee, D., & Boyle, E. A. (2020). A Lagrangian view of trace elements and isotopes in the North Pacific. *Journal of Geophysical Research: Oceans*, *125*, e2019JC015862. https://doi.org/10.1029/2019JC015862

Received 13 NOV 2019
Accepted 29 FEB 2020
Accepted article online 3 MAR 2020

Abstract Ocean time-series sites are influenced by both temporal variability, as in situ conditions change, as well as spatial variability, as water masses move across the fixed observation point. To remove the effect of spatial variability, this study made sub-daily Lagrangian observations of trace elements and isotopes (Al, Sc, Mn, Fe, Co, Ni, Cu, Zn, Cd, Pb, ^{232}Th, and ^{230}Th) in surface water over a 12-day period (July–August 2015) in the North Pacific near the Hawaii Ocean Time-series Station ALOHA. Additionally, a vertical profile in the upper 250 m was analyzed. This dataset is intercalibrated with GEOTRACES standards and provides a consistent baseline for trace element studies in the oligotrophic North Pacific. No diel changes in trace elements could be resolved, although day-to-day variations were resolved for some elements (Fe, Cu, and Zn), which may be related to organic matter cycling or ligand availability. Pb concentrations remained relatively constant during 1997–2015, presenting a change from previous decreases. Nutrient to trace element stoichiometric ratios were compared to those observed in phytoplankton as an indication of the extent of biological trace element utilization in this ecosystem, providing a basis for future ecological trace element studies.

1. Introduction

Eulerian observations in the ocean, that is, at a fixed location, can reflect the state of conditions in situ or the passage of mesoscale features across the site. The Hawaii Ocean Time-series (HOT) Station ALOHA (Karl & Church, 2019) (Figure 1) is a long-term time-series station but is known to be influenced by relatively short-lived circulation perturbations such as deep vertical mixing events, the passage of cyclonic eddies, Rossby waves, or the breaking of internal tides (Kavanaugh et al., 2018). Biogeochemical changes can be difficult to discern from spatial variability in this type of time series. For instance, Fitzsimmons et al. (2015) found that surface water dissolved Fe (dFe) concentrations at Station ALOHA could increase by nearly a factor of 4 within a few days, due to the passage of an anticyclonic eddy over the site. The effect of any in situ changes, such as changes to the biological use of iron or the input of iron from a dust event, are difficult to distinguish from these water mass changes.

Nonetheless, the question of biological use is at the forefront of trace element research in the ocean. Many trace elements, such as Fe, Mn, Zn, Ni, Cu, and Co, are known to be essential for biological processes in their form as metalloproteins (Morel & Price, 2003; Sunda, 2012) and in some cases can be inadequately supplied compared to phytoplankton demands (Moore, 2016). As clean sampling and analytical techniques have only recently been advanced and standardized (Anderson, 2020), there are relatively few time-series observations of trace elements with temporal resolution capable of addressing in situ variability or the stoichiometry of the suite of trace elements. This study addresses these issues, presenting a multielement data set collected using Lagrangian sampling, that is, from a ship following drifters to sample the same water mass consistently, in the well-studied oligotrophic North Pacific near Station ALOHA. Interestingly, intracellular usage of Fe, Ni, Zn, and Co inferred from gene expression was found to have clear diel variability on the same expedition (Frischkorn et al., 2018; Harke et al., 2019). This new trace metal dataset provides context for these and also future biogeochemical cycles in the North Pacific.

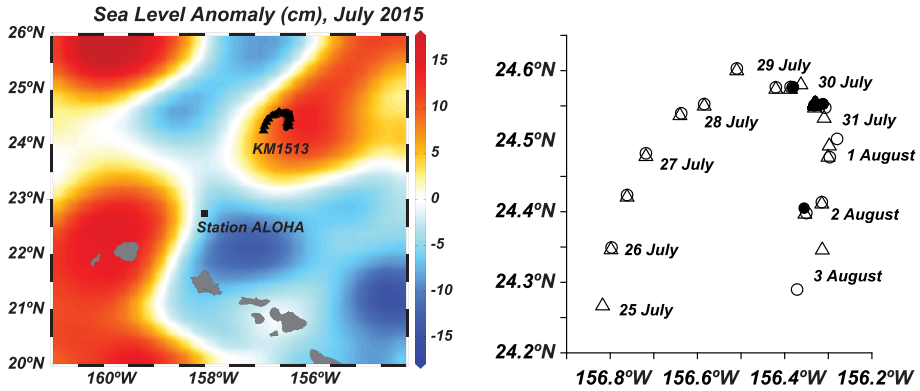

Figure 1. Map of station locations plotted from KM1513 (25 July to 3 August 2015), northeast of Station ALOHA, underlain by monthly mean sea level anomaly for July 2015 (left) derived from AVISO satellite altimetry, along with a detailed view of the sampling sites and dates (right). On the right, circles represent samplings for trace metals with the automated trace element (ATE) sampler. Triangles represent sampling for thorium isotopes from Niskin bottle casts or a surface water pump. Open symbols are mixed layer samples and filled symbols are depth profiles.

2. Materials and Methods

2.1. Field Work

Lagrangian sampling was performed on the R/V *Kilo Moana* (cruise number KM1513) over the course of 12 days in water representative of Station ALOHA in summer 2015. Prior to the expedition, AVISO satellite altimetry (Figure 1) was used to determine an appropriate starting point in the middle of a mesoscale eddy in order to maintain free drift within pelagic waters. An anticyclonic mode water eddy was chosen to deploy surface drifters roughly 86 nautical miles to the northeast of Station ALOHA, and the ship followed these drifters in a nearly complete clockwise rotation from 25 July to 4 August 2015 (Figure 1). For more information on fieldwork design, see Wilson et al. (2017). This expedition is known as Hawaii Ocean Experiment (HOE)-Legacy 2A of the SCOPE and C-MORE programs. This study also reports additional thorium isotope data from another C-MORE cruise to Station ALOHA in December 2014 (KM1427), known as HOE-Budget of Energy (BOE) 3.

This study also reports data from a longer term study of total dissolved Pb (tdPb) concentrations at Station ALOHA, updating that described by Boyle et al. (2005). Lead samples between 1997 and 2014 were collected from the Hawaii Air-sea Logging Experiment (HALE-ALOHA, 22° 28′N, 158° 8′W) mooring (1997–2000) and the Multi-disciplinary Ocean Sensors for Environmental Analyses and Networks (MOSEAN, 22° 46′ N, 158° 5.5′W) mooring (2004–2005), as well as shipboard sampling from over 50 of the monthly HOT (22° 45′N, 158° 00′W) occupations (1997–2012) and the C-MORE multicruise campaigns of HOE-Dynamics of Light and Nutrients (DYLAN) (2012) and HOE-Phosphorus Rally (PhoR) (2013).

2.2. Sampling and Analysis

CTD/Niskin casts to 400 m were performed every 4 hr on KM1513 for a variety of chemical and biological parameters. As the ship was following the surface drifter, each cast position was assigned a station number. There were 74 stations between 25 July and 4 August 2015. Macronutrients (phosphate, nitrate plus nitrite, and silicate) were analyzed on three depth profiles to 200 m at the beginning, middle, and end of the cruise (stations 5, 45, and 73 of KM1513), according to HOT protocols (Wilson et al., 2017). Nutrient and CTD data are archived by the University of Hawaii (http://hahana.soest.hawaii.edu/hoelegacy/data/data.html). Reported limits of detection for phosphate, nitrate plus nitrate, and silicate are 0.02, 0.03, and 0.3 μmol/kg, respectively (http://hahana.soest.hawaii.edu/hot/protocols/protocols.html). Corresponding precision values for the nutrients are 0.3%, 0.3%, and 6%, respectively.

Trace element water samples from KM1513 were collected with the MIT ATE sampler (Bell et al., 2002), deployed with a teflon-coated wire from the ship's deck for surface water samples (collected at roughly 10-m depth), and with the ATEs attached to PVC "Vanes" designed to prevent contamination from the ship's steel wire for samples collected at greater depth. Samples were filtered at 0.4 μm immediately after collection through polycarbonate track etched filters (Nucleopore) into 250-mL HDPE bottles and acidified with

hydrochloric acid (ultrapure by quadruple distillation in a Vycor still; final concentration 0.012 M ~ pH 2) at sea. Sampling and filtration followed published protocols used previously at Station ALOHA, for direct comparison (Fitzsimmons et al., 2015). These casts mostly aligned with Niskin cast station locations, but in some cases did not, and therefore, we reference the trace element sampling locations by their date/time (Figure 1).

Thorium isotope samples were collected from the ship's Niskin bottle rosette, and in some cases, surface water (from roughly 15-m depth) was also collected using a Teflon diaphragm pump (Cole Palmer) operated from the ship's deck. Water was filtered at 0.45 μm using Acropak filter cartridges and acidified to 0.024 M HCl (~pH 1.5) at sea.

Surface samples for both trace elements and thorium isotopes were taken every 12 hr between 25 July and 3 August, roughly at sunrise and sunset (Hawaii Standard Time). This timing was motivated to observe the maximum possible change in dissolved elemental concentrations since it coincides with the highest contrast in surface water biomass (maximum at sunset, minimum at sunrise) (A. E. White et al., 2017). Depth profile samples for trace elements were collected on 30 July at 10:00 a.m., except for the sample from 180 m, which was collected on 2 August at 4:00 p.m., due to a misfiring of the original 180 m Vanes deployment. Thorium depth profile samples were collected on 31 July at 2:00 a.m. (station 43 of KM1513).

Lead samples from 1997 to 2013 were collected using the MITESS (Moored In situ Trace Element Serial Sampler) moored sampler (1997–2005) and ATE shipboard sampling from HOT occupations (1997–2012), the HOE-DYLAN cruises (2012), and the HOE-PhoR cruises (2013). Samples from 1997 to 2000 were analyzed as described by Boyle et al. (2005) and samples after that by the method described by Lee et al. (2011). The 1997–2013 Pb samples were measured as tdPb, that is, analysis of an acidified unfiltered seawater sample. Since dissolved Pb (dPb) in pelagic settings is typically >90% of tdPb (Boyle et al., 2005), the tdPb concentrations from the Station ALOHA time series are directly comparable to the 2015 KM1513 dPb data, that is, filtered at 0.4 μm.

The elements Sc, Mn, Fe, Co, Ni, Cu, Zn, Cd, and Pb from the Lagrangian sampling (KM1513) were analyzed at Texas A&M University using an offline SeaFAST-pico preconcentration system (ESI, Omaha, NE) and a Thermo Finnigan Element XR high-resolution inductively coupled mass spectrometer (HR-ICP-MS) housed at the R. Ken Williams Radiogenic Isotope Facility. This is a modified version of published methods (Jensen et al., 2019; Lagerström et al., 2013). Notably, samples were not UV oxidized, and thus, cobalt concentrations must be considered to be operationally defined ICP-labile cobalt (lCo). Accuracy was assessed by analyzing aliquots of the SAFe D1 seawater consensus standard (Tables 1 and 2). Precision is shown via the error bars for each analysis and was assessed using the standard deviation of duplicate or triplicate analyses of all samples.

Thorium isotopes (^{232}Th and ^{230}Th) were analyzed at MIT by Fe co-precipitation from 4-L samples, acid digestion, anion exchange chromatography, and a Nu Plasma II ICP-MS. Protocols followed published methods (Hayes et al., 2015). Accuracy was assessed by analysis of the SWS2010-1 standard (Anderson et al., 2012) (Table 2) as well as an in-house thorium isotope standard (MITh-1). Reported uncertainty for thorium isotopes represents the uncertainty in isotope ratios measured on the ICP-MS.

Selected samples were also analyzed for dissolved aluminum (dAl) concentrations. These samples were subsampled from the water filtered from the ATE sampler, filtered directly into 125-mL acid washed PMP bottles and acidified to 0.006 M HCl and microwaved for 58 s/125 mL of sample. These samples were then acidified to 0.012 M HCl (~pH 2) and stored for shipboard analysis on a later cruise (R/V *Revelle* cruise RR1815 in November 2018) for dAl using flow injection analyses (Resing & Measures, 1994). Replicate standards were used to assess precision and accuracy of this method, and reported errors are the relative standard deviation of standard analyses.

3. Results

3.1. Hydrographic Context

Figures 2 displays temperature, fluorescence, and salinity from the cast closest in time to when depth profile samples were taken for trace elements and isotopes on 31 July 2015. Potential temperature and absolute salinity were derived using the Gibbs Seawater Oceanographic Toolbox (McDougal & Barker, 2011).

Table 1
Concentrations and Relative Standard Deviations of Trace Metal Measurements for the Bioactive Trace Metals of Surface Water Samples from KM1513 Versus Measurements of the SAFe D1 Seawater Standard

	dMn (nmol/kg)	dFe (nmol/kg)	lCo (pmol/kg)	dNi (nmol/kg)	dCu (nmol/kg)	dZn (nmol/kg)	dCd (pmol/kg)
Average surface water on KM1513 ($n = 16$) ± σ (%RSD)	1.04 ± 0.02 (1.8%)	0.43 ± 0.14 (31%)	40.2 ± 3.7 (9.1%)	2.30 ± 0.05 (2.1%)	0.80 ± 0.26 (33%)	0.42 ± 0.21 (50%)	1.04 ± 0.44 (42%)
Average of SAFe D1 standards ($n = 8$) ± σ (%RSD)	0.40 ± 0.02 (4.3%)	0.59 ± 0.07 (11%)	32.0 ± 1.7 (5.4%)	8.56 ± 0.16 (1.8%)	2.09 ± 0.18 (8.6%)	7.28 ± 0.20 (2.7%)	1030 ± 22 (2.2%)
Consensus values for SAFe D1 standards (2013) ± σ	0.35 ± 0.05[a]	0.67 ± 0.04	45.7 ± 2.9 (as dCo)	8.58 ± 0.26	2.27 ± 0.11	7.40 ± 0.35	991 ± 31

[a]For Mn, a consensus value for Mn was only available for the SAFe D2, which is assumed to be similar to D1.

The mixed layer, as defined by a 0.03 kg/m^3 offset in seawater density referenced to the 10 dbar isobar, was roughly 22 m from 25 July to 31 July and then deepened slightly to about 35 m between 31 July and 3 August (Wilson et al., 2017). These shallow mixed layers are typical of summertime conditions at Station ALOHA (Church et al., 2013). Mixed layer temperatures of 26.8 °C (Figure 2) were 1 °C warmer than the climatological mean due to the 2014–2016 El Niño (Wilson et al., 2017). The deep chlorophyll maximum was observed (via fluorescence, Figure 2) at 120-m depth, also typical of summer oligotrophic conditions at Station ALOHA (Letelier et al., 2004).

The observed nutrient profiles from KM1513 are shown in Figure 3 in the context of the mean, fifth percentile and 95th percentile values from all of the HOT time-series observations (1988–2017, http://hahana.soest.hawaii.edu/index.html). Binned depth zones were 0–10, 11–50, 51–100, 101–150, and 151–200 m. For the historical data, each depth zone had between 600 and 1,200 measurements. Nutrient profiles observed on KM1513 were close to the long-term mean. Nitrate plus nitrite was below detection (<0.03 μmol/kg) from the surface to the nitricline observed at around 100-m depth. The upper 180 m was characterized by phosphate and silicate levels of about 0.1 and 1 μmol/kg, respectively. Within the precision of the methods, the only significant change in time in nutrient concentrations was observed at 150-m depth or greater (Figure 3).

3.2. Vertical Trace Element Profiles

Dissolved iron (dFe) is one of the most heavily studied trace elements at Station ALOHA, and the dFe depth profile from this study can be put into context of many prior observations collected between 1994 and 2013. In the upper 250 m of the water column, we compiled 126 published dFe measurements (Boyle et al., 2005; Fitzsimmons et al., 2015; Rue & Bruland, 1995) and depth-binned them to take mean, fifth and 95th percentile values for each bin. The binned depth zones were as follows, with the number of observations available in parenthesis: 0–10 ($n = 65$), 11–50 ($n = 17$), 51–100 ($n = 13$), 101–150 ($n = 11$), 151–200 ($n = 8$), 201–250 (n = 8), and 251–323 m ($n = 4$). The KM1513 dFe profile, with mixed layer dFe of about 0.4 nmol/kg declining to 0.2 nmol/kg at the deep chlorophyll maximum around 130 m, is close to the long-term mean profile (Figure 4). This was previously attributed to dust inputs of Fe to the surface ocean, combined with biological uptake through the deep chlorophyll maximum (Fitzsimmons et al., 2015). The higher dFe concentrations at

Table 2
Concentrations and Relative Standard Deviations of Trace Metal Measurements for the Abiotic Metals of Surface Water Samples from KM1513 Versus Measurements of the SAFe D1 (Pb, Sc) and SWS2010-1 (Th isotopes) Seawater Standards

	dPb (pmol/kg)	dSc (pmol/kg)	d^{232}Th (fmol/kg)	d^{230}Th (μBq/kg)
Average surface water on KM1513 (n = 16) ± σ (%RSD)	26.1 ± 1.1 (4%)	1.9 ± 0.5 (25%)	51.4 ± 3.5 (7%)	0.64 ± 0.14 (22%)
Average of SAFe D1 or SWS2010–1 standards (n = 8) ± σ (%RSD)	22.9 ± 1.6 (7%)	6.4 ± 1.1 (17%)	4195 ± 124 (3%)	179 ± 8 (4%)
Consensus values for standards ± σ	27.7 ± 2.6	11.4 ± 0.6*	4234 ± 44	180 ± 2

Note. There is no consensus value for dissolved Sc in SAFe D1 and instead reported with the * is the value reported at 1,000 m from the SAFe site by Parker et al. (2016). Thorium concentrations for SWS2010-1 are from Anderson et al. (2012).

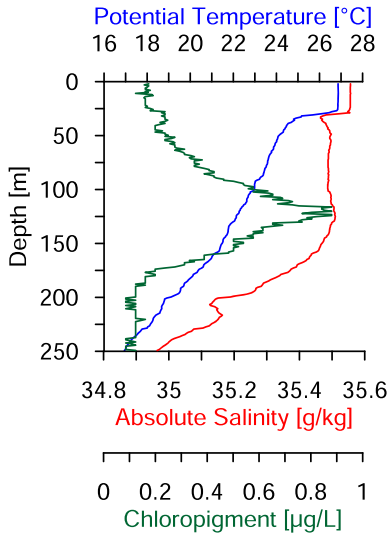

Figure 2. Vertical CTD profiles (station 45 of KM1513) from 31 July 2015 7:54 p.m. This cast was closest in time to when vertical profiles were analyzed for trace elements and isotopes. Blue curve is potential temperature, red is absolute salinity, and green is chloropigment (chlorophyll-a as well as other pigments contributing to measured fluorescence).

180 m (0.758 nmol/kg; not plotted in Figure 4) and 250 m (0.646 nmol/kg) during KM1513 are outside of the previously observed range. The 180-m sample also appeared contaminated for dZn, but not any other elements including dPb. Sample contamination can never be completely ruled out, and therefore we treat the 180-m dFe value with caution.

The dissolved cadmium (dCd) profile resembled the shape of the nitrate profile, with very low concentrations of about 1 pmol/kg from the surface to a depth of about 100 m and a rapid increase to 35 pmol/kg at 250-m depth (Figure 4). While no prior concentration measurements of dCd have been reported at Station ALOHA, similarly low surface water concentrations of dCd have been reported at the SAFE site (30°N, 140°W) (Biller & Bruland, 2012; Conway & John, 2015) and the VERTEX-IV site (28°N, 155°W) (Bruland et al., 1994) (see Figure 5 for locations). The extremely low surface dCd concentrations are illustrative of the strongly oligotrophic conditions of the subtropical North Pacific. However, the concentrations of dCd match those expected based on phosphate concentrations, as was reported for the North Pacific and extended to the rest of the global ocean (Boyle et al., 1976; Bruland et al., 1978; Cullen, 2006). This is best encapsulated using the concept of Cd*, which is defined as the measured dCd minus an expected dCd based on measured phosphate multiplied by the cadmium to phosphate ratio in deep water (Conway & John, 2015). There was constant, near-zero Cd* (0.02 to −0.03 nmol/kg) between the surface and deep chlorophyll maximum of KM1513, which indicates that euphotic zone dCd falls within the range expected based on surface phosphate concentrations and deep remineralized Cd/P ratios; these Cd* values are also well aligned with the near-zero Cd* observed at nearby SAFe previously (Conway & John, 2015; all calculated using a deep Cd/P of 0.317 nmol/µmol).

Labile cobalt (lCo) also displayed a nutrient-like profile, more similar in shape to phosphate than nitrate (Figures 3 and 4). Upper water column lCo concentrations, increasing from 3 to 13 pmol/kg with depth in the upper 250 m, are similar to dissolved Co (dCo) concentrations reported from Station ALOHA (Morton et al., 2019) and the SAFe site (Biller & Bruland, 2012), and to lCo concentrations from nearby station KH05-2-St. 8 (26.3°N, 160°W) (Zheng et al., 2019). KM1513 lCo concentration are, however, lower than dCo reported from the E-flux study (10 to 40 pmol/kg) that made observations in mesoscale eddies in oceanographic waters west of the big island of Hawaii and south of Maui (Noble et al., 2008) (see Figure 5 for locations). It was proposed that the continental shelf of the Hawaiian Islands could be a major source of cobalt to the surrounding waters (Noble et al., 2008; Pinedo-González et al., 2015). The conclusion of a strong shelf influence on cobalt distributions in the open North Pacific was also reached from a large section study

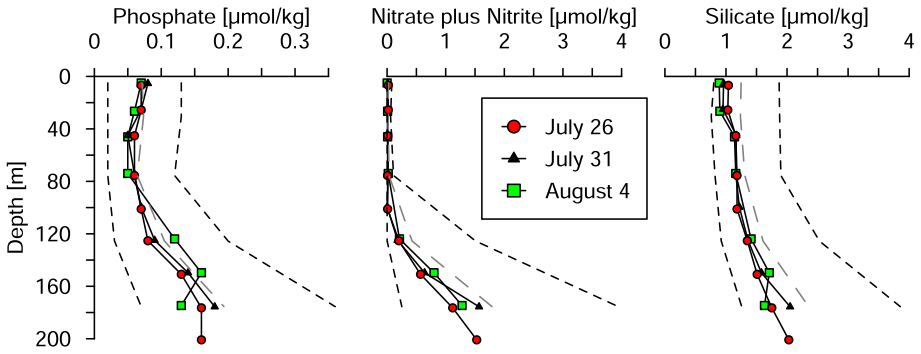

Figure 3. Nutrient profiles from KM1513. Three profiles were taken at the beginning, middle, and end of the expedition, on July 26 (red circles), July 31 (black triangles), and August 4 (green squares) 2015, respectively, shown in solid symbols and lines. Phosphate (left), nitrate plus nitrite (center), and silicate (right). The gray, long dashed line for each is the mean profile from all measurements made a station ALOHA between 1988 and 2017. The short dashed lines are the fifth and 95th percentiles of the values within binned depth zones of the 1988–2017 dataset.

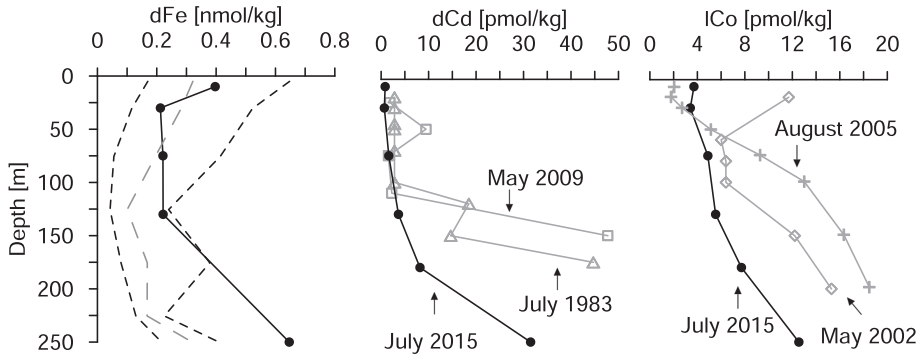

Figure 4. Dissolved trace metal profiles from KM1513 (July 2015) showing nutrient-like profiles (black circles). Dissolved Fe (left) is shown with the mean (long dash) and fifth and 95th percentile values of all dissolved Fe measurements made at Station ALOHA (1994–2013) (Boyle et al., 2005; Fitzsimmons et al., 2015; Rue & Bruland, 1995). Dissolved Cd (center) is shown with prior data from other North Pacific sites: VERTEX-IV (July 1983; gray diamonds; Bruland et al., 1994), SAFe (May 2009; gray squares; Biller & Bruland, 2012). Labile Co (right) from KM1513 is shown with prior dissolved Co data from Station ALOHA (May 2002; gray diamonds; Morton et al., 2019) and from lCo data from KH05-2 St. 8 (August 2005; gray crosses; Zheng et al., 2019). Note the KM1513 sample from 180 m appeared contaminated for Fe (0.758 nmol/kg) and is not plotted.

carried out along 160°W in 2005 (Zheng et al., 2019). We explain our relatively lower lCo near Hawaii as either (1) a function of lCo-dCo differences in the presence of elevated shelf cobalt influences from the Hawaiian Islands or (2) a function of lower cobalt supply from the Hawaiian Islands due to the farther distance (and North Pacific eddy influence) of our KM1513 sampling site.

Dissolved manganese (dMn) in KM1513 had maximum concentrations of ~1.0 nmol/kg in the upper 75 m, and declining concentrations with depth to 0.5 nmol/kg at 250 m (Figure 5). This profile shape is a well-known "scavenging type" distribution, indicating surface input likely due to atmospheric deposition and perhaps photochemical reduction and subsequent scavenging at depth (Klinkhammer & Bender, 1980; Landing & Bruland, 1980). There have been prior profiles of dMn determined at Station ALOHA (Boyle et al., 2005; Chen & Wu, 2019; Morton et al., 2019) as well as at several other stations in the proximity including VERTEX-IV (July 1983), SAFe (May 2009), and KH05-2-9 and KH05-2-8 (April 2005) (Zheng et al., 2019) (see Figure 5 for locations). We binned the profiles from these sites to compare the KM1513 results to a mean, fifth and 95th percentile profile (Figure 5) The binned depth zones were as follows, with the number of observations available in parenthesis: 0–10 (n = 11), 11–50 (n = 20), 51–100 (n = 13), 101–150 (n = 6), 151–200 (n = 6), 201–250 (n = 4), and 251–300 m (n = 4). The KM1513 dMn profile was close to the mean profile from the 0- to 150-m depth and somewhat higher than the mean between 175 and 250 m, although there are fewer observations in the mean at these depths. Higher surface water dMn

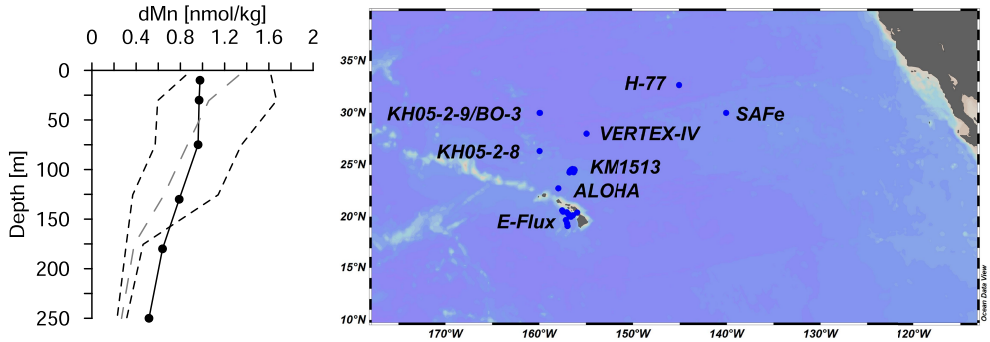

Figure 5. (Left) dissolved Mn depth profiles from KM1513 (July 2015) shown with the mean (long dash) and fifth and 95th percentile values (short dash) of numerous dMn measurements made at Station ALOHA (Boyle et al., 2005; Chen & Wu, 2019; Morton et al., 2019) as well as several other stations in the regional North Pacific including the VERTEX-IV (July 1983), SAFe (May 2009) and KH05-2-9 and KH05-2-8 (April 2005) (Zheng et al., 2019). Additional station locations mentioned in the text for other elements are also plotted in the map on the right.

(~1.5 nmol/kg) than KM1513 was clearly observed in the 2005 Hawaiian Islands E-flux study (see Figure 5 for locations) (Noble et al., 2008). It is likely the islands are a source of Mn to the surrounding surface water in all of these more nearshore studies. It is possible that changes in the production or transport of this island source could cause subdecadal changes in Mn concentrations in the proximity of the Hawaiian Islands, as Mn is known to have a short residence time of 2.5 years in surface water (Hayes et al., 2018). Furthermore, island-sourced trace metals are more likely to be transported toward the northwest of the Hawaiian Islands than the northeast due to North Hawaiian Ridge Current that runs from the southeast to the northwest along the Hawaiian Ridge (Qiu et al., 1997; W. White, 1983).

Dissolved zinc (dZn), nickel (dNi), and copper (dCu) concentrations did not display significant trends in profile (Figure 6), with means and standard deviations of the 250 m profiles being 0.24 ± 0.12 (50% RSD) nmol/kg, 2.34 ± 0.09 (3.8% RSD) nmol/kg, and 0.52 ± 0.06 (12% RSD) nmol/kg, respectively. For zinc, these KM1513 concentrations are similar to those reported for the SAFe (Biller & Bruland, 2012; Conway & John, 2015) and VERTEX-IV (Bruland et al., 1994) sites. They also show a classically similar distribution to dissolved silicate. Similar to Cd*, we utilize the Zn* concept defined by Conway and John (2015), which is defined as measured dZn minus expected dZn based on measured silicate multiplied by a deep water zinc to silicate ratio. Zn* values in KM1513 increased from 0.03 nmol/kg at the surface to 0.32 nmol/kg at the deep chlorophyll maximum, within range of the 0–0.5 nmol/kg observed at the SAFe site previously (Conway & John, 2015; both calculated using deep Zn/Si of 0.056 nmol/μmol). Similar surface water dNi concentrations of 2–3 nmol/kg and dCu concentrations of 0.5–1.0 nmol/kg are also seen across the mid-latitude North Pacific (Biller & Bruland, 2012; Boyle et al., 1981; Bruland, 1980).

Dissolved lead (dPb) in surface seawater was first measured near Station ALOHA (24°19′N, 154°29′W) in 1977 at 63.7 pmol/kg (tdPb was also measured at 65.6 pmol/kg at that station with similar levels further to the northeast; Schaule & Patterson, 1981). Martin et al. (1985) reported a somewhat lower value from surface water at the VERTEX-IV site collected in 1983 of 41.7 pmol/kg Pb. Boyle et al. (2005) reported concentrations similar to or lower than these levels at Station ALOHA during 1997–1999, measuring tdPb levels from an automated moored sampler ranging from 24 to 56 pmol/kg (median 33 pmol/kg). Here, we extend this time series to 2015 using MOSEAN moored sampler data (2004–2005), HOT ATE sampler data, and C-MORE ATE sampler data from 2002 to 2015 (Figure 7; Boyle, 2020). Total dissolvable lead levels for 2002–2015 (24–51 pmol/kg, median 30 pmol/kg) fluctuated within nearly the same range as 1997–1999. Additionally, in an annual climatology of the 1997–2015 Pb data, the lowest tdPb concentrations typically occurred in summer (Figure 7), the timing of the July 2015 sampling. The decline from the 1970's observations can be attributed to the phase-out of leaded gasoline in North America and Japan, although this was a less drastic decline than that observed in the Atlantic due to phase-out of leaded gasoline in North American and Europe (Boyle et al., 2014; Pinedo-González et al., 2018). Interestingly, tdPb was slightly higher at 60- to 100-m depth at Station ALOHA in May 2002 than in May 1999 (Zurbrick et al., 2017) (Figure 8).

Dissolved scandium (dSc) and thorium-232 ($d^{232}Th$) are both abiotic indicators of continental dust input to the ocean, as well as metal scavenging by adsorption on to particles (Hayes, Anderson, Fleisher, et al., 2013; Till et al., 2017) and can serve as abiotic analogues of the bioactive metals such as Fe. Dissolved Sc displayed profiles of about 2 pmol/kg with a slight minimum of 1.5 pmol/kg at 75- to 125-m depth (Figure 8). These levels are similar to the 0.8 to 3.2 pmol/kg dSc measured at the SAFe site (Parker et al., 2016) and the BO-3 site (Amakawa et al., 2007) (Figure 5 for locations) in the upper 200 m of the water column. The profile shape is similar to that of the $d^{232}Th$, which is suggestive of atmospheric dust flux and enhanced scavenging near the depths of the deep chlorophyll maximum (Figure 8). The KM1513 profile of $d^{232}Th$ is close to the mean profile from measurements between 1994 and 2014 (Hayes et al., 2015; Roy-Barman et al., 1996), including a previously unreported profile collected in December 2014 on KM1427 (see Hayes, 2020), in the upper 125 m. Depth bins and number of observations in this case are 0–10 m (n = 26), 11–50 m (n = 7), 51–100 m (n = 4), 101–150 m (n = 4), 151–200 m (n = 4), and 248 to 252 m (n = 4). Values of about 30 fmol/kg $d^{232}Th$ at 175- and 250-m depth are lower than previously observed. The average Sc/Th molar ratio in the upper 250 m is 52 mol/mol, while the average for the upper continental crust is 6.9 (Rudnick & Gao, 2014). Thus, the seawater appears enriched in Sc with respect to Th, assuming an upper continental crust source and congruent dissolution of Sc and Th, by factor of about 7. This factor is close to the ratio of residence times of Sc and Th, derived by Hayes et al. (2018) in Atlantic surface water of 5.2 (10.3 year surface water residence time for Sc and 2 year surface water residence time for Th). Therefore, Sc and Th are likely

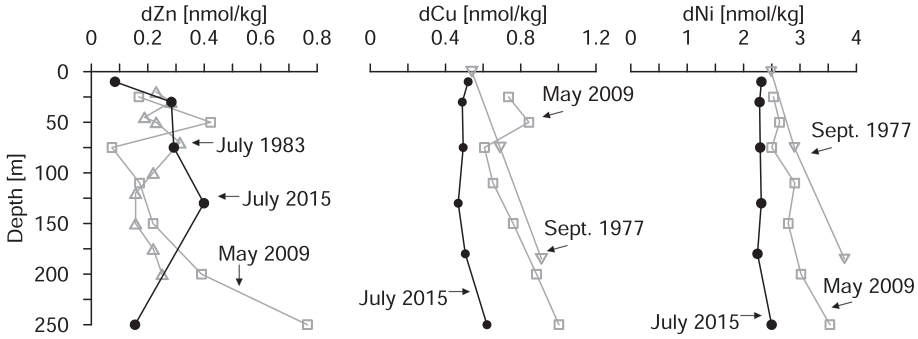

Figure 6. (Left) Dissolved Zn from KM1513 (July 2015; black circles) compared with that from the VERTEX-IV site (July 1983) (Bruland et al., 1994) and the SAFe site (May 2009) (Biller & Bruland, 2012). (Center) Dissolved Cu from KM1513 (July 2015; black circles) compared with that from site H-77 (September 1977) (Bruland, 1980) and the SAFe site (May 2009) (Biller & Bruland, 2012). (Right) Dissolved Ni from KM1513 (July 2015; black circles) compared with that from H-77 (September 1977) (Bruland, 1980) and SAFe (May 2009) (Biller & Bruland, 2012). Note the KM1513 sample from 180 m appeared contaminated for Zn (1.26 nmol/kg) and is not plotted.

both good indicators of continental input to the ocean, but Sc is scavenged less intensely than Th and its water column concentration will be averaged over longer timescales.

Dissolved thorium-230 ($d^{230}Th$), the long-lived product of decay of dissolved uranium and a well-known scavenging tracer (Hayes, Anderson, Jaccard, et al., 2013), was also measured in profile on KM1513 (see Supplemental Data). This occupation was found to be very similar to the profile measured in July 2012 (Hayes et al., 2015), with about 0.6 μBq/kg in the upper 250 m.

3.3. Lagrangian Surface Water Time Series

Figure 9 displays the 12-hr resolution, Lagrangian time-series observations of dMn, dFe, lCo, dNi, dCu, dZn, and dCd on KM1513, presented in order of atomic number. One way to assess the magnitude of temporal variability for different metals is to compare the relative standard deviation of all surface water

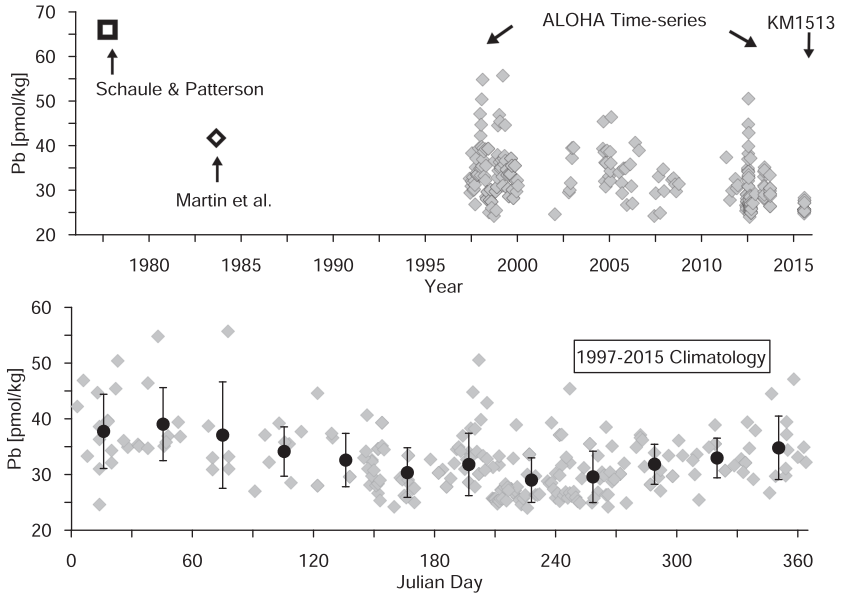

Figure 7. (Top) Near-surface (~10-m depth) total dissolvable Pb data near Hawaii collected between 1977 and 2015. The open box point was reported by Schaule and Patterson (1981) and the open diamond point was reported by Martin et al. (1985). Of the gray diamond points from Station ALOHA, Boyle et al. (2005) reported data up until year 2000, and new data is reported here from 2000 to 2015, year 2015 data being the KM1513 expedition. (Bottom) The data from 1997 to 2015 (gray diamonds) were collapsed onto 1 annual cycle, ordered by Julian Day, and the black circles represent the mean and standard deviations of the monthly climatology.

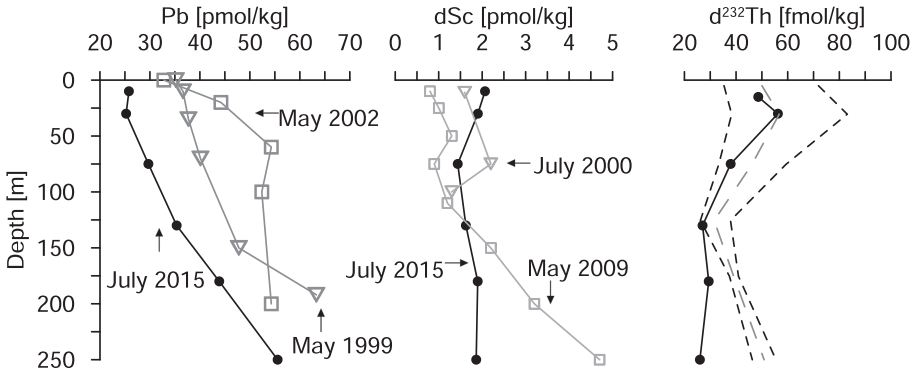

Figure 8. (Left) Pb profiles from KM1513 (July 2015, black circles) compared with previous depth profile measurements from Station ALOHA in 1999 and 2002 (Boyle et al., 2005; Zurbrick et al., 2017). The 1999 and 2002 data were collected from unfiltered water samples, while the 2015 samples were filtered at 0.4 μm. (Center) Dissolved Sc from KM1513 compared with previous measurements from the SAFe site (Parker et al., 2016) and from site BO-3 (Amakawa et al., 2007). (right) dissolved thorium-232 from KM1513 compared with the average depth-binned profile (long dashed) of all thorium-232 measurements made at Station ALOHA (1994–2014), with the fifth and 95th percentiles shown in short dashed lines (Hayes et al., 2015; Roy-Barman et al., 1996).

measurements in the time series to the relative standard deviation of replicate standards measured made during the analyses (Table 1). For Mn, Co, and Ni, the relative standard deviation of the sample measurements was smaller or similar (less than a factor of 2) to that of the standard measurements, indicating little to no resolvable variations in the surface water concentrations over time at Station ALOHA. For Fe, Cu, and Zn, the opposite appears to be the case with sample relative standard deviation well above (more than a factor of 2) that of the standard measurements. In case of Cd, Station ALOHA surface water concentrations are much lower than the deep water standard (1 pmol/kg vs. 991 pmol/kg), and in this case, the absolute standard deviation of the standard is larger than the variation seen the samples. The ~1 pmol/kg dCd levels are close to the detection limit of the method (0.6 pmol/kg), and therefore, we do not interpret this as clear, daily-scale variation in Cd.

For dFe, dCu, and dZn, for which there does appear to be discernible Lagrangian variation during KM1513, no statistically significant ($p < 0.05$) diel difference was found. This was assessed using a 2-tailed t test between sunset and sunrise concentrations. Therefore, biological uptake during the day does not appear to be the main influence on dissolved metal concentration variations in this case. This is somewhat surprising since on this same cruise, *Trichodesmium*, a common diazotroph at Station ALOHA in summertime, was observed to show daytime-peaking expression of Fe-containing proteins such as photosystem electron transport proteins and nitrogenase (Frischkorn et al., 2018). However, this diel variability was not observed in dFe concentrations at the surface. Instead, the range seen in dFe concentrations is similar to that seen in daily level observations made in summer 2012 (Fitzsimmons et al., 2015), even after removing the spatial variability influences involved in those prior Eulerian observations. While sample contamination cannot be ruled out, dFe cycling appears to remain dynamic at short timescales, perhaps with cycles of longer than 1 day. Hourly observations using a continuous sensor may be required to determine the cause of these short time scale concentration variations, which may apply for Cu and Zn as well as Fe.

None of these elements displayed a statistically significant ($p < 0.05$) trend with time, based on Pearson correlation between concentrations and time. With 16 observations, the Pearson's r correlation coefficient must be 0.498 or greater for the $p < 0.05$ significance level. We also ran a cross-correlation analysis between the trace element time series. The only pair of elements whose time series were significantly ($p < 0.05$) correlated were Cu and Zn (Pearson's $r = 0.606$). Some common features at certain time points do stand out for Cu, Zn, and Fe, the three elements that showed the greatest temporal variability. For example, all three appear to have relatively high values on 28 July starting in the evening. Between 29 July and 3 August, dCu remains relatively constant whereas both dFe and dZn have slightly increasing concentrations for the remainder of the cruise (between 31 July and 3 August; Figure 9). While the cause of this variation is still unclear, we discuss the possible influence of three factors: mixed layer deepening, biological remineralization or ligand availability in section 4.

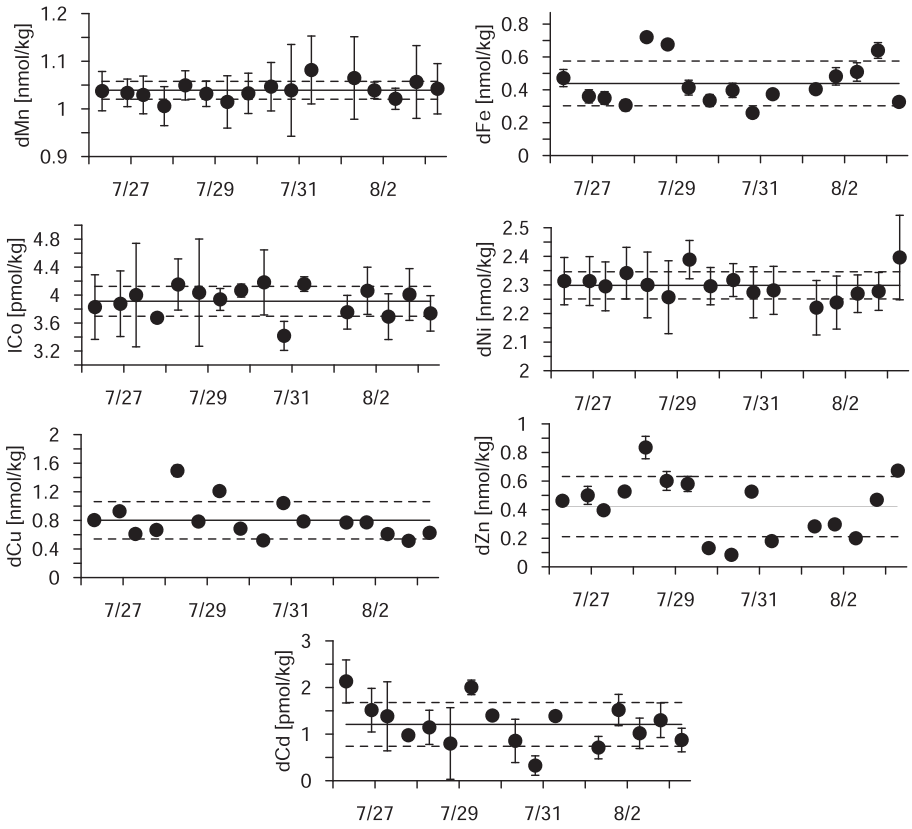

Figure 9. High temporal resolution surface water sampling of trace metals (left to right from top) for dissolved Mn and Fe, labile Co, and dissolved Ni, Cu, Zn, and Cd on KM1513 in July–August 2015. Samplings are spaced roughly at every sunrise and sunset. Where error bars are not visible they are smaller than the symbol size. Also shown are the mean (solid line) and ±1 standard deviation (dotted lines) of each data set.

Finally, the subdaily time series from KM1513 of the suite of the abiotic scavenging-type metals is shown in Figure 10. The variability in dissolved Pb, Sc, ^{232}Th, and ^{230}Th over the course of the cruise was similar to that derived from replicate standard measurements (Table 2), and therefore, we do not interpret any significant temporal changes over the course of the time series. In the case of thorium isotopes, the samples have a larger relative standard deviation than that of standards, indicating a slight decrease in both isotope concentrations over the course of the cruise. However, the seawater thorium standard (SWS2010-1) has much higher concentrations of both isotopes, and the absolute standard deviations of standards are larger than the apparent trend of thorium isotopes, and thus, we do not consider this significant.

A subset of the surface water samples was also analyzed for dAl (between 1 and 3 August, $n = 5$; Figure 10). The goal of these analyses was to provide an additional comparison for the lithogenic tracers Sc and Th. Al is a major component of the continental crust and has been used extensively as a tracer for dust in the North Pacific (e.g., Measures et al., 2005). The average and standard deviation of dAl was 4.2 ± 1.1 nmol/kg. We do not interpret the statistical variation due to the small size of this subset; however, it can be noted that these dAl concentrations are similar to the 2–3 nmol/kg dAl found in the upper 75 m at the SAFe site in 2009 (Parker et al., 2016) and in the upper 200 m at a site near Station ALOHA in 2005 (26.4°N, 160°W) (Zheng et al., 2019). In contrast, these 2015 Station ALOHA observations are lower than measurements of dAl at Station ALOHA in previous decades. Han et al. reported 8–16 nmol/kg dAl in surface water at Station ALOHA throughout the year during 1994–1997 (Han et al., 2008) and Measures et al. (2005) reported 5–6 nmol/kg in May 2002, in addition to a strong island effect of elevated dAl coming from Kauai island (Measures et al., 2005). These observations fit with those made previously for Mn (section 3.2) and Co. It may be that the location of the KM1513 is further away from island effects from the Hawaiian Islands than Station ALOHA and perhaps more specifically due to the northwesterly track of the North Hawaiian Ridge Current.

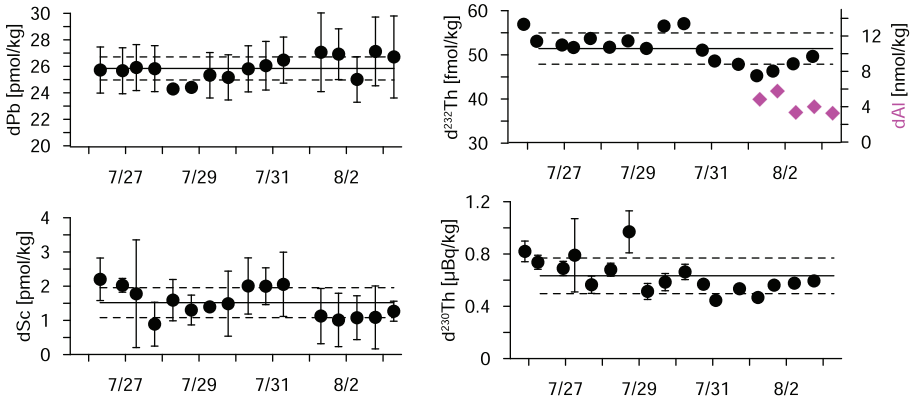

Figure 10. High temporal resolution surface water sampling of (left to right from top) dissolved Pb, dissolved thorium-232 (circles) overlain with dissolved Al (magenta diamonds), dissolved Sc and dissolved thorium-230. Also shown are the mean (solid line) and ±1 standard deviation (dotted lines) of the data sets, with the exception of Al.

4. Discussion

4.1. Fe and Zn Variability During KM1513

We address three possibilities for the increase found for dissolved Zn and Fe in the latter half of KM1513, 31 July to 3 August (Figure 11).

First, a very slight mixed layer deepening was observed throughout the cruise (based on a 0.03 kg/m^3 density offset from 10 dbar pressure; Wilson et al., 2017). Mixed layer depths deepened from about 20 m from 27 to 30 July, increasing to about 35 m by August 3 (Figure 11). In the depth profile, taken on 31 July, the 10-m sample was 0.08 nmol/kg dZn and at 30 m was 0.28 nmol/kg dZn, meaning that entrainment of deeper water into the mixed layer would have increased mixed layer dZn concentrations (Figure 6). In contrast, dFe concentrations decreased from 0.40 nmol/kg to 0.21 nmol/kg over the same depth range, suggesting that entrainment of deeper water into the mixed layer would have decreased dFe concentrations (Figure 4). Thus, this deepening mixed layer explanation is insufficient to explain the temporal trend, as both dZn and dFe increased similarly at the surface over the 30 July to 3 August time period (Figure 11).

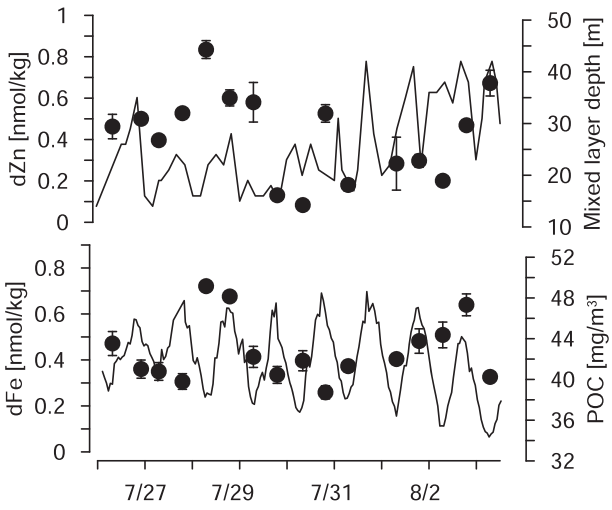

Figure 11. High temporal resolution surface water sampling of dissolved Zn (circles, top panel) and dissolved Fe (circles, bottom panel) compared against changes to the mixed layer depth (solid line, top panel; Wilson et al., 2017) and against particulate organic carbon concentration (solid line, bottom panel; White et al., 2017) in the bottom panel.

A second possibility is that grazing of a phytoplankton bloom released biogenic zinc and iron back into the water column. Iron and zinc are the two metals with highest abundances in cellular stoichiometry (Twining & Baines, 2013), and thus, they are most prone of the trace metals to respond to internal biological cycling changes, especially in oligotrophic areas where their surface inventories are already low. White et al. (2017) reconstructed surface water particulate organic carbon (POC) concentrations with hourly resolution during KM1513 using transmissometry on an underway seawater flow-through system. POC concentrations, with clear diel variability, slightly declined between 31 July and 3 August (Figure 11), suggestive of a net loss of organic matter and subsequent remineralization of the biogenic material. As Wilson et al. (2017) describe, the KM1513 observation period was characterized by bloom conditions for the cyanobacterium *Crocosphaera*, which at the time was the second most abundant cyanobacterium in terms of biomass (after *Prochlorococcus*). Throughout the course of KM1513, large-celled *Crocosphaera* (>4 μm) decreased consistently, which may have been related to grazing pressure or viral lysis (Wilson et al., 2017), potentially conducive to release of excess iron and zinc. Surface water macronutrients were not measured with sufficient resolution to test for increasing values over the course of the cruise and the macronutrient data that were collected were close to the mean historical values (Figure 3), rather than

on the high end of the range which might be expected during a significant remineralization event. On the other hand, surface water POC concentrations had a diel variability of roughly 10 mg/m^3, or 0.83 μmol/kg (Figure 11). Using estimates of remineralized dFe/C ratios of 2.5 to 3.1 μmol/mol from analysis of dFe and AOU at Station ALOHA (Fitzsimmons et al., 2015), the diel POC change would suggest 2.1–2.6 nmol/kg Fe being remineralized (cf. average surface water dFe of ~0.5 nmol/kg). Thus, there is strong potential for remineralization to impact the surface water dFe, and we conclude there is not enough information available to reject this explanation.

A third possibility is that both dissolved Fe and Zn are being similarly controlled by the availability of the ligands that help stabilize the metals in solution. During cruise KOK1507, which occurred simultaneously with KM1513 (http://hahana.soest.hawaii.edu/hoelegacy/data/data.html), strong organic Fe-binding ligands concentrations were in excess of dFe in a profile between 0- and 400-m depth (Bundy et al., 2018). Additionally, iron ligands have been shown to be variable on daily timescales at Station ALOHA (Fitzsimmons et al., 2015). Dissolved zinc is also known to be 98% organically complexed, for example, at the VERTEX-IV site (Bruland, 1989). Bruland et al. (2014) discussed the concept of "smart banking" for zinc in which some phytoplankton species may intentionally release chelating ligands to make zinc less bioavailable overall but when needed reduced ligand production could be advantageously timed. It is possible that ligand production for zinc and iron could be intentionally or coincidentally coordinated in the case of KM1513 and that ligand availability dominated the temporal changes in the dissolved metals.

We consider possibilities 2 and 3 to be plausible causes of the largest variations seen in dissolved Fe and Zn (and perhaps Cu) on KM1513. Future work to help constrain this issue could include sensor-based continuous metal measurements, complementary high resolution sampling of metal ligands, and/or further comparison of the dominant phytoplankton species and the production rates of specific metal co-factors (e.g., Saito et al., 2011). Deployable in situ observing systems for marine micronutrients are beginning to be developed (Grand et al., 2019). With adequate sampling frequency for Fourier transforms, frequency analyses could be performed to resolve daily or longer cycles that are hinted at in our data. Continued time-series studies at locations such as ALOHA and BATS, with their wealth of baseline information, will push forward our understanding of marine trace metal dynamics.

4.2. Bioactive Metal:Nutrient Stoichiometry

One of the reasons that this dataset is unique is because of its high-resolution sampling within a Lagrangian water mass, removing the influence of spatial hydrographic variability and allowing a detailed assessment of biological influences. While diel micronutrient changes remain elusive, we can still use the dataset as a snapshot of the nutrient stoichiometry in seawater of the oligotrophic North Pacific. In Table 3, we calculated the average and standard deviation of dissolved metal to phosphorous (as phosphate) ratios within the depth profile measurements through 130 m of the water column, approximately at and shallower than the deep chlorophyll maximum. Thus, this is the pool against which phytoplankton will draw when taking up nutrients for cellular function. By comparing these ratios dissolved in seawater with those measured within phytoplankton cells themselves, one can get a sense of the relative scarcity of the trace metals with respect to their need. As nitrogen is the scarcest nutrient at Station ALOHA (e.g., Figure 3), diazotrophic nitrogen fixation is likely ultimately limited by P and/or Fe availability (Letelier et al., 2019). Co-limitations or secondary limitations of particular metabolic processes by other trace metals are also possible (Moore, 2016).

For this comparison, we draw from the metal to phosphorus ratios derived by Twining and Baines (2013) who estimated phytoplankton composition from a variety of methods. These methods included elemental analysis of cultured phytoplankton or bulk marine particles, synchrotron X-ray fluorescence analysis of phytoplankton cells, or large-scale regressions of dissolved metal to nutrient ratios in seawater. The estimates of phytoplankton composition ratios often range over 1 to 2 orders of magnitude. Nonetheless, comparing that range with the well-constrained dissolved ratios measured during KM1513 is still instructive. Cobalt was not included in this analysis due to the uncertainties relating to dissolved versus labile forms.

The dissolved metal to phosphorus ratios in KM1513 seawater are within the range of observed phytoplankton composition for Fe, Zn, and Cd (Table 3). In contrast, metal to phosphorus ratios for Mn, Ni, and Cu during KM1513 are well above the maximum observed in phytoplankton. One interpretation of this result is that some biological processes may approach limitation by availability of Fe, Zn, or Cd in the subtropical North

Table 3
Metal to Phosphorus Ratios (mmol:mol)

	Fe	Zn	Mn	Ni	Cu	Cd
Dissolved (KM1513, upper 130 m)	3.6 ± 1.2	3.6 ± 1.7	12.8 ± 3.6	31.5 ± 6.6	6.8 ± 1.5	0.020 ± 0.012
Dissolved (greater North Pacific, <800 m) (Twining & Baines, 2013)	0.5 ± 0.3	3.9 ± 1.2	Not available	1.0 ± 0.1	0.41 ± 0.8	0.40 ± 0.11
Observed range in phytoplankton (Twining & Baines, 2013)	0.1–20	0.2–16	0.2–4.0	0.2–1.8	0.2–2.0	0.01–2.0

Pacific. Notably, the range found for Fe:P in cells by Twining and Baines (2013) was 0.1 to 20 mmol/mol compared to the 3.6 mmol/mol found in the surface water in this study, indicating that conditions may have been on the lower side of Fe supply compared to demand. Insufficient iron supply may have been more significant for diazotrophs specifically that were present in our region at the time of KM1513. In fact, *Trichodesmium* was observed during the daytime hours of KM1513 to express flavodoxin, an Fe-free protein that is substituted for ferredoxin, its Fe-intensive analogue, under conditions of Fe stress (Frischkorn et al., 2018). Furthermore, a recent culturing study focusing on the cyanobacteria that dominate phytoplankton populations at Station ALOHA found Fe/P ratios even higher than 20 mmol/mol up to 78 mmol/mol under iron replete conditions (Cunningham & John, 2017), highlighting the relatively low seawater ratio observed at KM1513. Further study of phytoplankton composition relevant to the subtropical North Pacific will provide more detailed evidence for any trace metal deficiencies.

In contrast, it appears resources of Mn, Ni, and Cu in this region are well in excess of biological-need based on our dissolved-to-phytoplankton comparison. One factor leading to this situation may in fact be the limitation of biological uptake by other trace metals or macronutrients. Twining and Baines (2013) also compiled available seawater data on trace metal:phosphorus ratios in the North Pacific (Table 3) and the KM1513 ratios are also relatively enriched in Ni and Cu compared to that compilation of the North Pacific (see references in Twining & Baines, 2013). In the global analysis by Moore (2016), it was found the Mn is not typically limiting at low latitudes, in agreement with our results, and the greatest evidence for Mn limitation was from Southern Ocean surface waters. Diverging from our findings, prior work has found evidence for Cu limitation, as well as toxicological, effects in the subarctic Pacific (e.g., Coale, 1991; Semeniuk et al., 2009). Future work may benefit from further dissecting the reasons for different Cu and/or Ni regimes between the subtropical and subarctic Pacific. Station ALOHA and the Lagrangian snapshot data provided in this study provide a well-constrained basis for further study of ecological trace element impacts.

5. Conclusions

In this study, Lagrangian observations of trace elements and isotope concentrations (Al, Sc, Mn, Fe, Co, Ni, Cu, Zn, Cd, Pb, ^{232}Th, and ^{230}Th) were made in surface water in the North Pacific near Station ALOHA every 12 hr over a 12-day period (July–August 2015). This study was innovative in its diel temporal resolution within a single water mass, strategically removing the effects of spatial variability in the temporal trends. Surprisingly, no diel changes in trace elements could be resolved, even for micronutrients involved in diel enzymatic processes, although day-to-day variations were resolved for some elements (Fe, Cu, and Zn), which may have been related to daily changes in organic matter cycling or ligand production. A longer term surface time series (1977–2015) of surface water Pb was also presented and showed declining anthropogenic lead concentrations between historical measurements in 1977 and 1997–1999, but relatively constant, interannual variability between 1999 and 2015. The Hawaiian Islands appear to be a source of Al, Mn, and Co to the regional North Pacific and more so at Station ALOHA than to the northeast of it at KM1513, perhaps due to steering influence of the northwesterly North Hawaiian Ridge Current. Nutrient to trace element ratios were compared against the same ratios reported for phytoplankton. Levels of dissolved Fe and Zn appear to be close to limiting levels in the subtropical North Pacific during summer 2015, while it appeared that supplies of Mn, Ni, and Cu were relatively replete. This intercalibrated dataset provides a new, multielement baseline for trace element studies in the oligotrophic North Pacific at a well-studied time-series site.

Acknowledgments

Funding for this study was provided by the Center for Microbial Oceanography: Research & Education (NSF-OIA Award EF-0424599), the Simons Collaboration on Ocean Processes and Ecology (SCOPE), the University of Southern Mississippi, Texas A&M University, and the U.S. National Science Foundation (award nos. 1737023 to CTH, NSF 1737167 to JNF, 1736906 to MH, and NSF Graduate Research Fellowship 1746932 to NTL). Thanks to Randie Bundy and Dan Repeta for collection of thorium samples on KM1427, to Sam Wilson for cruise leadership on KM1513, and to the crew and captain of the R/V *Kilo Moana*. Thanks to Rick Kayser for ATE preparation and Jing Zhang for some lead data from HOT. We acknowledge Ben Twining and an anonymous reviewer for constructive comments that improved the manuscript. New data reported here are archived at BCO-DMO (https://www.bco-dmo.org/dataset/792817 and https://www.bco-dmo.org/dataset/792783).

References

Amakawa, H., Nomura, M., Sasaki, K., Oura, Y., & Ebihara, M. (2007). Vertical distribution of scandium in the north central Pacific. *Geophysical Research Letters*, *34*, L11606. https://doi.org/10.1029/2007GL029903

Anderson, R. F. (2020). GEOTRACES: Accelerating research on the marine biogeochemical cycles of trace elements and their isotopes. *Annual Review of Marine Science*, *12*, 9.1–9.37. https://doi.org/10.1146/annurev-marine-010318-095123

Anderson, R. F., Fleisher, M. Q., Robinson, L. F., Edwards, R. L., Hoff, J. A., Moran, S. B., et al. (2012). GEOTRACES intercalibration of ^{230}Th, ^{232}Th, ^{231}Pa, and prospects for ^{10}Be. *Limnology and Oceanography: Methods*, *10*(4), 179–213. https://doi.org/10.4319/lom.2012.10.179

Bell, J., Betts, J., & Boyle, E. (2002). MITESS: A moored in situ trace element serial sampler for deep-sea moorings. *Deep-Sea Research Part I*, *49*(11), 2103–2118. https://doi.org/10.1016/S0967-0637(02)00126-7

Biller, D. V., & Bruland, K. W. (2012). Analysis of Mn, Fe, Co, Ni, Cu, Zn, Cd, and Pb in seawater using the Nobias-chelate PA1 resin and magnetic sector inductively coupled plasma mass spectrometry (ICP-MS). *Marine Chemistry*, *130–131*, 12–20. https://doi.org/10.1016/j.marchem.2011.12.001

Boyle, E. A. (2020). Surface water total dissolvable lead concentrations near Station ALOHA from 1997 to 2013. Biological and Chemical Oceanography Data Management Office (BCO-DMO), Dataset version 2020-02-11. https://doi.org/10.1575/1912/bco-dmo.792783.1

Boyle, E. A., Bergquist, B. A., Kayser, R. A., & Mahowald, N. (2005). Iron, manganese, and lead at Hawaii Ocean Time-series station ALOHA: Temporal variability and an intermediate water hydrothermal plume. *Geochimica et Cosmochimica Acta*, *69*(4), 933–952. https://doi.org/10.1016/j.gca.2005.03.006

Boyle, E. A., Huested, S., & Jones, S. P. (1981). On the distribution of copper, nickel, and cadmium in the cadmium based on mum observed at GEOSECS station jot processes controlling their distributions the of the mixed is difficult to contaminate and is low these were face by organisms into the maximum. *Journal of Geophysical Research*, *86*, 8048–8066. https://doi.org/10.1029/JC086iC09p08048

Boyle, E. A., Lee, J. M., Echegoyen, Y., Noble, A., Moos, S., Carrasco, G., et al. (2014). Anthropogenic lead emissions in the ocean: The evolving global experiment. *Oceanography*, *27*(1), 69–75. https://doi.org/10.5670/oceanog.2014.10

Boyle, E. A., Sclater, F., & Edmond, J. M. (1976). On the marine geochemistry of cadmium. *Nature*, *263*, 42–44. https://doi.org/10.1038/263042a0

Bruland, K. W. (1980). Oceanographic distributions of cadmium, zinc, nickel, and copper in the North Pacific. *Earth and Planetary Science Letters*, *47*, 176–198. https://doi.org/10.1016/0012-821X(80)90035-7

Bruland, K. W. (1989). Complexation of cadmium by natural organic ligands in the central North Pacific. *Limnology and Oceanography*, *34*(5), 269–285. https://doi.org/10.4319/lo.1989.34.2.0269

Bruland, K. W., Knauer, G. A., & Martin, J. N. (1978). Cadmium in northeast Pacific waters. *Limnology and Oceanography*, *23*(4), 618–625. https://doi.org/10.4319/lo.1978.23.4.0618

Bruland, K. W., Middag, R., & Lohan, M. C. (2014). Controls of trace metals in seawater. In H. D. Holland & K. K. Turekian (Eds.), *Treatise on Geochemistry* (2nd ed., Vol. 8, pp. 19–51). New York: Elsevier. https://doi.org/10.1016/B978-0-08-095975-7.00602-1

Bruland, K. W., Orians, K. J., & Cowen, J. P. (1994). Reactive trace metals in the stratified central North Pacific. *Geochimica et Cosmochimica Acta*, *58*(15), 3171–3182. https://doi.org/10.1016/0016-7037(94)90044-2

Bundy, R. M., Boiteau, R. M., McLean, C., Turk-Kubo, K. A., McIlvin, M. R., Saito, M. A., et al. (2018). Distinct siderophores contribute to iron cycling in the mesopelagic at station ALOHA. *Frontiers in Marine Science*, *5*, 1–15. https://doi.org/10.3389/fmars.2018.00061

Chen, G., & Wu, J. (2019). Meridional distribution of dissolved manganese in the tropical and equatorial Pacific. *Geochimica et Cosmochimica Acta*. https://doi.org/10.1016/j.gca.2019.06.048

Church, M. J., Lomas, M. W., & Muller-Karger, F. (2013). Sea change: Charting the course for biogeochemical ocean time-series research in a new millennium. *Deep-Sea Research Part II*, *93*, 2–15. https://doi.org/10.1016/j.dsr2.2013.01.035

Coale, K. H. (1991). Effects of iron, manganese, and zinc enrichments on productivity and biomass in the subarctic Pacific. *Limnology and Oceanography*, *36*(8), 1851–1864. https://doi.org/10.4319/lo.1991.36.8.1851

Conway, T. M., & John, S. G. (2015). The cycling of iron, zinc and cadmium in the North East Pacific Ocean—Insights from stable isotopes. *Geochimica et Cosmochimica Acta*, *164*, 262–283. https://doi.org/10.1016/j.gca.2015.05.023

Cullen, J. T. (2006). On the nonlinear relationship between dissolved cadmium and phosphate in the modern global ocean: Could chronic iron limitation of phytoplankton growth cause the kink? *Limnology and Oceanography*, *51*(3), 1369–1380. https://doi.org/10.4319/lo.2006.51.3.1369

Cunningham, B. R., & John, S. G. (2017). The effect of iron limitation on cyanobacteria major nutrient and trace element stoichiometry. *Limnology and Oceanography*, *62*(2), 846–858. https://doi.org/10.1002/lno.10484

Fitzsimmons, J. N., Hayes, C. T., Al-Subiai, S. N., Zhang, R., Morton, P. L., Weisend, R. E., et al. (2015). Daily to decadal variability of size-fractionated iron and iron-binding ligands at the Hawaii Ocean Time-series Station ALOHA. *Geochimica et Cosmochimica Acta*, *171*. https://doi.org/10.1016/j.gca.2015.08.012

Frischkorn, K. R., Haley, S. T., & Dyhrman, S. T. (2018). Coordinated gene expression between Trichodesmium and its microbiome over day-night cycles in the North Pacific subtropical gyre. *ISME Journal*, *12*(4), 997–1007. https://doi.org/10.1038/s41396-017-0041-5

Grand, M. M., Laes-Huon, A., Fietz, S., Resing, J. A., Obata, H., Luther, G. W., et al. (2019). Developing autonomous observing systems for micronutrient trace metals. *Frontiers in Marine Science*, *6*(35), 1–17. https://doi.org/10.3389/fmars.2019.00035

Han, Q., Moore, J. K., Zender, C., Measures, C., & Hydes, D. (2008). Constraining oceanic dust deposition using surface ocean dissolved Al. *Global Biogeochemical Cycles*, *22*, GB2003. https://doi.org/10.1029/2007GB002975

Harke, M. J., Frischkorn, K. R., Haley, S. T., Aylward, F. O., Zehr, J. P., & Dyhrman, S. T. (2019). Periodic and coordinated gene expression between a diazotroph and its diatom host. *ISME Journal*, *13*(1), 118–131. https://doi.org/10.1038/s41396-018-0262-2

Hayes, C. T. (2020). Surface and profile concentrations of trace metals and radionuclides near Station ALOHA. Biological and Chemical Oceanography Data Management Office (BCO-DMO), dataset version [2020-02-11]. https://doi.org/10.1575/1912/bco-dmo.792817.1

Hayes, C. T., Anderson, R. F., Cheng, H., Conway, T. M., Edwards, R. L., Fleisher, M. Q., et al. (2018). Replacement times of a spectrum of elements in the North Atlantic based on thorium supply. *Global Biogeochemical Cycles*, *32*(9), 1294–1311. https://doi.org/10.1029/2017GB005839

Hayes, C. T., Anderson, R. F., Fleisher, M. Q., Serno, S., Winckler, G., & Gersonde, R. (2013). Quantifying lithogenic inputs to the North Pacific Ocean using the long-lived thorium isotopes. *Earth and Planetary Science Letters*, *383*, 16–25. https://doi.org/10.1016/j.epsl.2013.09.025

Hayes, C. T., Anderson, R. F., Jaccard, S. L., François, R., Fleisher, M. Q., Soon, M., & Gersonde, R. (2013). A new perspective on boundary scavenging in the North Pacific Ocean. *Earth and Planetary Science Letters*, *369–370*, 86–97. https://doi.org/10.1016/j.epsl.2013.03.008

Hayes, C. T., Fitzsimmons, J. N., Boyle, E. A., McGee, D., Anderson, R. F., Weisend, R., & Morton, P. L. (2015). Thorium isotopes tracing the iron cycle at the Hawaii Ocean Time-series Station ALOHA. *Geochimica et Cosmochimica Acta*, *169*, 1–16. https://doi.org/10.1016/j.gca.2015.07.019

Jensen, L. T., Wyatt, N. J., Twining, B. S., Rauschenberg, S., Landing, W. M., Sherrell, R. M., & Fitzsimmons, J. N. (2019). Biogeochemical cycling of dissolved zinc in the Western Arctic (Arctic GEOTRACES GN01). *Global Biogeochemical Cycles*, *33*(3), 343–369. https://doi.org/10.1029/2018GB005975

Karl, D. M., & Church, M. J. (2019). Station ALOHA: A gathering place for discovery, education, and scientific collaboration. *Limnology and Oceanography Bulletin*, *28*(1), 10–12. https://doi.org/10.1002/lob.10285

Kavanaugh, M. T., Church, M. J., Davis, C. O., Karl, D. M., Letelier, R. M., & Doney, S. C. (2018). ALOHA from the edge: Reconciling three decades of in situ Eulerian observations and geographic variability in the North Pacific subtropical gyre. *Frontiers in Marine Science*, *5*, 1–14. https://doi.org/10.3389/fmars.2018.00130

Klinkhammer, G. P., & Bender, M. L. (1980). The distribution of manganese in the Pacific Ocean. *Earth and Planetary Science Letters*, *46*(3), 361–384. https://doi.org/10.1016/0012-821X(80)90051-5

Lagerström, M. E., Field, M. P., Séguret, M., Fischer, L., Hann, S., & Sherrell, R. M. (2013). Automated on-line flow-injection ICP-MS determination of trace metals (Mn, Fe, Co, Ni, Cu and Zn) in open ocean seawater: Application to the GEOTRACES program. *Marine Chemistry*, *155*, 71–80. https://doi.org/10.1016/j.marchem.2013.06.001

Landing, W. M., & Bruland, K. W. (1980). Manganese in the North Pacific. *Earth and Planetary Science Letters*, *49*, 45–56. https://doi.org/10.1016/0012-821X(80)90149-1

Lee, J. M., Boyle, E. A., Echegoyen-Sanz, Y., Fitzsimmons, J. N., Zhang, R., & Kayser, R. A. (2011). Analysis of trace metals (Cu, Cd, Pb, and Fe) in seawater using single batch nitrilotriacetate resin extraction and isotope dilution inductively coupled plasma mass spectrometry. *Analytica Chimica Acta*, *686*(1–2), 93–101. https://doi.org/10.1016/j.aca.2010.11.052

Letelier, R. M., Björkman, K. M., Church, M. J., Hamilton, D. S., Mahowald, N. M., Scanza, R. A., et al. (2019). Climate-driven oscillation of phosphorus and iron limitation in the North Pacific subtropical gyre. *Proceedings of the National Academy of Sciences, USA*, *116*(26), 12,720–12,728. https://doi.org/10.1073/pnas.1900789116

Letelier, R. M., Karl, D. M., Abbott, M. R., & Bidigare, R. R. (2004). Light driven seasonal patterns of chlorophyll and nitrate in the lower euphotic zone of the North Pacific subtropical gyre. *Limnology and Oceanography*, *49*(2), 508–519. https://doi.org/10.4319/lo.2004.49.2.0508

Martin, J., Knauer, G., & Broenkow, W. (1985). VERTEX: The lateral transport of manganese in the northeast Pacific. *Deep Sea Research*, *32*(11), 1405–1427. https://doi.org/10.1016/0198-0149(85)90056-1

McDougal, T. J., & Barker, P. M. (2011). Getting started with TEOS-10 and the Gibbs Seawater (GSW) Oceanographic Toolbox. SCOR/IAPSO WG127.

Measures, C. I., Brown, M. T., & Vink, S. (2005). Dust deposition to the surface waters of the western and central North Pacific inferred from surface water dissolved aluminum concentrations. *Geochemistry, Geophysics, Geosystems*, *6*, Q09M03. https://doi.org/10.1029/2005GC000922

Moore, C. M. (2016). Diagnosing oceanic nutrient deficiency. *Philosophical Transactions of the Royal Society A*, *374*, 20,150,290. https://doi.org/10.1098/rsta.2015.0290

Morel, F. M. M., & Price, N. M. (2003). The biogeochemical cycles of trace metals. *Science (New York, N.Y.)*, *300*, 944–947. https://doi.org/10.1126/science.1083545

Morton, P. L., Landing, W. M., Shiller, A. M., Moody, A., Kelly, T. D., Bizimis, M., et al. (2019). Shelf inputs and lateral transport of Mn, Co, and Ce in the Western North Pacific Ocean. *Frontiers in Marine Science*, *6*. https://doi.org/10.3389/fmars.2019.00591

Noble, A. E., Saito, M. A., Maiti, K., & Benitez-Nelson, C. R. (2008). Cobalt, manganese, and iron near the Hawaiian Islands: A potential concentrating mechanism for cobalt within a cyclonic eddy and implications for the hybrid-type trace metals. *Deep-Sea Research Part II*, *55*(10–13), 1473–1490. https://doi.org/10.1016/j.dsr2.2008.02.010

Parker, C. E., Brown, M. T., & Bruland, K. W. (2016). Scandium in the open ocean: A comparison with other group 3 trivalent metals. *Geophysical Research Letters*, *43*, 2758–2764. https://doi.org/10.1002/2016GL067827

Pinedo-González, P., West, A. J., Tovar-Sánchez, A., Duarte, C. M., Marañón, E., Cermeño, P., et al. (2015). Surface distribution of dissolved trace metals in the oligotrophic ocean and their influence on phytoplankton biomass and productivity. *Global Biogeochemical Cycles*, *29*, 1763–1781. https://doi.org/10.1002/2015GB005149

Pinedo-González, P., West, A. J., Tover-Sanchez, A., Duarte, C. M., & Sañedo-Wilhemy, S. A. (2018). Concentration and isotopic composition of dissolved Pb in surface waters of the modern global ocean. *Geochimica et Cosmochimica Acta*, *235*, 41–54. https://doi.org/10.1016/j.gca.2018.05.005

Qiu, B., Koh, D. A., Lumpkin, C., & Flament, P. (1997). Existence and formation mechanism of the north Hawaiian ridge current. *Journal of Physical Oceanography*, *27*, 431–444. https://doi.org/10.1175/1520-0485(1997)027<0431:EAFMOT>2.0.CO;2

Resing, J. A., & Measures, C. I. (1994). Fluorometric determination of Al in seawater by flow injection analysis with in-line preconcentration. *Analytical Chemistry*, *66*, 4105–4111. https://doi.org/10.1021/ac00094a039

Roy-Barman, M., Chen, J. H., & Wasserburg, G. J. (1996). ^{230}Th-^{232}Th systematics in the central Pacific Ocean: The sources and fates of thorium. *Earth and Planetary Science Letters*, *139*, 351–363. https://doi.org/10.1016/0012-821X(96)00017-9

Rudnick, R. L., & Gao, S. (2014). Composition of the Continental Crust. In H. D. Holland & K. K. Turekian (Eds.), *Treatise on Geochemistry* (2nd ed., Vol. 4, pp. 1–51). New York: Elsevier. https://doi.org/10.1016/B978-0-08-095975-7.00301-6

Rue, E. L., & Bruland, K. W. (1995). Complexation of iron (III) by natural organic ligands as determined by a new competitive equilibration/adsorptive cathodic stripping voltammetry method. *Marine Chemistry*, *50*, 117–139. https://doi.org/10.1016/0304-4203(95)00031-L

Saito, M. A., Bertrand, E. M., Dutkiewicz, S., Bulygin, V. V., Moran, D. M., Monteiro, F. M., et al. (2011). Iron conservation by reduction of metalloenzyme inventories in the marine diazotroph Crocosphaera watsonii. *Proceedings of the National Academy of Sciences, USA*, *108*(6), 2184–2189. https://doi.org/10.1073/pnas.1006943108

Schaule, B. K., & Patterson, C. C. (1981). Lead concentrations in the northeast Pacific: Evidence for global anthropogenic perturbations. *Earth and Planetary Science Letters*, *54*, 97–116. https://doi.org/10.1016/0012-821X(81)90072-8

Semeniuk, D. M., Cullen, J. T., Johnson, W. K., Gagnon, K., Ruth, T. J., & Maldonado, M. T. (2009). Plankton copper requirements and uptake in the subarctic Northeast Pacific Ocean. *Deep-Sea Research Part I*, *56*(7), 1130–1142. https://doi.org/10.1016/j.dsr.2009.03.003

Sunda, W. G. (2012). Feedback interactions between trace metal nutrients and phytoplankton in the ocean. *Frontiers in Microbiology*, *3*, 1–22. https://doi.org/10.3389/fmicb.2012.00204

Till, C. P., Shelley, R. U., Landing, W. M., & Bruland, K. W. (2017). Dissolved scandium, yttrium, and lanthanum in the surface waters of the North Atlantic: Potential use as an indicator of scavenging intensity. *Journal of Geophysical Research: Oceans*, *122*, 1–14. https://doi.org/10.1002/2017JC012696

Twining, B. S., & Baines, S. B. (2013). The trace metal composition of marine phytoplankton. *Annual Review of Marine Science*, *5*(1), 191–215. https://doi.org/10.1146/annurev-marine-121211-172322

White, A. E., Barone, B., Letelier, R. M., & Karl, D. M. (2017). Productivity diagnosed from the diel cycle of particulate carbon in the North Pacific subtropical gyre. *Geophysical Research Letters*, *44*, 3752–3760. https://doi.org/10.1002/2016GL071607

White, W. (1983). A narrow boundary current along the eastern side of the Hawaiian ridge; the north Hawaiian ridge current. *Journal of Physical Oceanography*, *13*, 1726–1731. https://doi.org/10.1175/1520-0485(1983)013<1726:ANBCAT>2.0.CO;2

Wilson, S. T., Aylward, F. O., Ribalet, F., Barone, B., Casey, J. R., Connell, P. E., et al. (2017). Coordinated regulation of growth, activity and transcription in natural populations of the unicellular nitrogen-fixing cyanobacterium *Crocosphaera*. *Nature Microbiology*, *2*(9), 17118. https://doi.org/10.1038/nmicrobiol.2017.118

Zheng, L., Minami, T., Konagaya, W., Chan, C. Y., Tsujisaka, M., Takano, S., et al. (2019). Distinct basin-scale-distributions of aluminum, manganese, cobalt, and lead in the North Pacific Ocean. *Geochimica et Cosmochimica Acta*, *254*, 102–121. https://doi.org/10.1016/j.gca.2019.03.038

Zurbrick, C. M., Gallon, C., & Flegal, A. R. (2017). Historic and industrial lead within the Northwest Pacific Ocean evidenced by lead isotopes in seawater. *Environmental Science and Technology*, *51*(3), 1203–1212. https://doi.org/10.1021/acs.est.6b04666